JOURNAL OF COMPUTATIONAL PHYSICS 94, 284–313 (1991)

Nonlinear Fourier Analysis for the Infinite-Interval Korteweg–de Vries Equation I: An Algorithm for the Direct Scattering Transform

A. R. OSBORNE

Istituto di Fisica Generale dell'Università and Istituto di Cosmo-Geofisica del C.N.R., Via Pietro Giuria 1, Torino 10125, Italy

Received June 6, 1989; revised November 14, 1989

The nonlinear Fourier analysis of wave motion governed approximately by the Korteweg–de Vries (KdV) equation on the infinite line is the central point of discussion. We assume that the wave amplitude is recorded in the form of a discrete space or time series which is determined either by experimental measurement or by computer simulation of the physical system of interest. We develop numerical data analysis procedures based upon the scattering transform solution to the KdV equation as given by Gardner *et al.* [1]. We are motivated by the observation that historically the Fourier transform has been ubiquitously used to spectrally analyze linear wave data; here we develop methods for employing the scattering transform as a tool to similarly analyze nonlinear wave data. Specifically we develop numerical methods to evaluate the direct scattering transform (DST) of a space or time series: the approach thus provides a basis for analyzing and interpreting nonlinear wave behavior in the wavenumber or frequency domain. The DST spectrum separates naturally into soliton and radiation components and may be simply interpreted in terms of the large-time asymptotic state of the infinite-line KdV equation.

1. INTRODUCTION

The study of the physics of wave motion has historically benefited from analytical, numerical, and experimental exploitation of the linear *Fourier transform* (FT) (Ablowitz and Segur [1], Bendat and Piersol [2, 3]). One reason for the wide applicability of this method is that many *linear partial differential equations* (i.e., linear wave equations, LWEs) may be solved exactly using Fourier methods. Thus while most physical systems are nonlinear, the fact that a closely related linear system may be exactly solvable by the Fourier transform often provides key insight. An important intermediate step in these calculations is the appearance of the Fourier wavenumber of frequency spectrum. While the wave motion itself may be a rather complicated function of time, the time evolution of the Fourier spectrum for linear wave motion is quite simple: *the Fourier amplitudes are constants, while the phases vary sinusoidally* ($e^{i\omega t}$). Because of this simple behavior, the Fourier spectrum is often viewed as more fundamental than the wave motion itself, e.g., the Fourier components constitute the *normal modes* of the system. Furthermore, given

0021-9991/91 $3.00

the Fourier spectrum and the dispersion relation (easily found from the LWE) the wave motion is known for all time and is represented as a *linear superposition of the sinusoidal normal modes.*

In the last 20 years there has been considerable progress in the understanding of certain nonlinear wave equations (NLWEs). Beginning with the work of Gardner, Greene, Kruskal, and Miura [4], who found the exact solution to the Korteweg–de Vries equation on the infinite interval for a suitably localized initial wave, a major revolution has occurred in mathematical physics. Solutions to entire classes of NLWEs on the infinite interval have been found [1, 4–12] (these include, in particular, the KdV, nonlinear Schroedinger, sine-Gordon, and modified KdV equations) and the methods have been christened the inverse scattering transform (IST). It can be shown that IST is a nonlinear generalization of the Fourier transform [1, 5]. Several wave equations are now known to have solutions not only on the infinite interval, but also on the periodic domain as well (these include the KdV [13, 14], nonlinear Schroedinger [15] and sine-Gordon equations [16]). These periodic solutions have been shown to be nonlinear generalizations of Fourier series [17–20]. Certain discrete wave equations on the infinite line (continuous in time, discrete in space) also have exact solutions given by the ST: [21] (see [1] for a review). One of the key features of the ST is that it approaches the Fourier transform in the small amplitude, linear limit; in this way the ST solution covers not only the nonlinear problem but also the associated linearized problem as well.

Given the availability of these new mathematical methods, in analogy with historical use of the Fourier transform, we have suggested that the ST be applied to the study of various problems in nonlinear wave physics [22–30]. The feature which we have exploited is that the direct scattering transform (DST) is a wavenumber representation of a nonlinear signal (assumed governed by some NLWE) just as the direct Fourier transform (DFT) is a wave number representation of a linear signal. One advantage of the DST is that it provides a spectral representation of the wave motion at one (singular-perturbative) order of approximation higher than the associated linear problem and, hence, one order of approximation higher than the linear Fourier transform. Thus one is "closer" (in the wavenumber domain) to the actual nonlinear physics of a particular system. Using this idea we have conducted preliminary nonlinear spectral analyses of wave data from the ocean [25, 29] and the laboratory [28].

Application of the algorithm developed herein has led to the resolution of the Zabusky and Kruskal problem [19, 20], which addresses how infinite-line solitons are related to solitons on the periodic domain. Other investigators have studied periodic spectral problems for the Toda lattice [30], and the sine–Gordon and nonlinear Schroedinger equations [31]. These important papers have considered nonlinear problems with a small number of excited degrees of freedom (i.e., nonlinear Fourier modes); this contrasts with the present series of papers which emphasizes the study of systems which may range up to several thousand degrees of freedom.

This paper has been written not only to give the development of an algorithm for

the DST but also to provide the reader with the tools for rapid implementation of the procedure and for understanding the physical implications of its use. We do not assume that the reader is an expert in scattering transform theory. The paper is the first in a series of papers which describes computer algorithms which we loosely call "nonlinear signal processing methods." These are based upon both infinite-interval and periodic ST theory for the KdV equation. The methods are analogous to the well-known linear signal processing techniques for the Fourier transform. We emphasize three principal operations of the algorithms:

(1) *Generation of a wavenumber (or frequency) domain spectrum.* Given a computer-generated signal or a measured space or time series of some localized or periodic wave motion, compute the direct scattering transform (DST); i.e., generate the wavenumber (or frequency) space representation of the input signal.

(2) *Filtering.* The inverse scattering transform (IST) is the inverse of the DST operation; i.e., the IST reconstructs the signal given the DST spectrum. In order to filter a signal of certain wavenumber or frequency components one first eliminates from the spectrum the unwanted components and then the nonlinear, filtered signal is reconstructed with the IST.

(3) *Time evolution.* The wave motion may be evolved forward or backward in time t simply by selecting the value of t desired and then executing the IST algorithm. The output of the IST operation is the signal advanced to the specified time. In the filtering operation of (2) above, the time t is normally taken to be zero.

This paper (I) is the first in a series which discusses algorithms for computing the direct and inverse scattering transforms for both the whole-line and periodic KdV equations. The infinite-interval DST algorithm is presented herein and numerical tests and an error analysis are given in II. A restricted nonlinear filtering algorithm, designed to extract the soliton component from a time series, is discussed in II. The infinite-interval IST is addressed in III. Generalized nonlinear filtering on the infinite line is also discussed in III, with several concrete examples given to illustrate the method. The DST and IST for the periodic KdV equation are developed in subsequent papers [32].

The rest of this paper is organized as follows. In Section 2 we review the Fourier transform solution to the linearized KdV equation. These results provide a basis for discussing the scattering transform solution to the KdV equation on the infinite interval (Section 3). The relationship between the linear Fourier transform and the scattering transform is discussed in Section 4, where particular emphasis is placed on those results necessary for development of the numerical algorithm for the DST, and for physically interpreting nonlinear wave motion governed by the KdV equation. Section 5 reviews some of the important assumptions leading to discrete Fourier methods; Section 6 discusses how we modify and elaborate on these to develop a set of assumptions which the DST algorithm must satisfy. In Section 7 we conclude that a need exists for a new algorithm which more nearly meets these requirements set forth in Section 6. To develop such an algorithm we describe in

Sections 8 and 9 the exact DST for a piecewise constant initial wave form which is partitioned at equal spatial intervals Δx; the result is a pseudo-discretization of the eigenvalue problem associated with the DST. Section 10 shows how the discrete DST solution may be simplified so that it depends only on Δx rather than x itself. This resolves certain problems with "exploding exponential" solutions which often occur in the discrete (soliton) spectrum; roundoff error is reduced to tolerable levels and computed numbers stay within the range of most computers. In Section 11 we develop recursion relations which allow for rapid machine calculation of the DST. Finally in Section 12 we discuss how the DST algorithm approaches the discrete Fourier transform in the small amplitude limit.

2. The Fourier Transform Solution to the Linearized KdV Equation

One can describe the approximate motion of infinitesimal amplitude, long dispersive waves in shallow water by the linearized KdV equation (set $\alpha = 0$ in Eq. (3.1) below):

$$\eta_t + c_0 \eta_x + \beta \eta_{xxx} = 0. \tag{2.1}$$

We write the equation in dimensional form, where $\eta(x, t)$ is the amplitude of the free surface, $c_0 = (gh)^{1/2}$ is the linear phase speed, g is the acceleration of gravity, h is the water depth, and $\beta = c_0 h^2/6$ is the constant coefficient of the dispersive term. Subscripts refer to partial derivatives with respect to space x or time t. Equation (2.1) is written in laboratory coordinates and has the dispersion relation

$$\omega = k(c_0 - \beta k^2). \tag{2.2}$$

The KdV equation ((3.1) below) and its linearized form (2.1) appear in many other physical contexts (see Chap. 4 of [1]). The constant coefficients change their form depending upon the physics of the problem; to apply the spectral analysis techniques in this paper one uses constants suitable for a particular application or one rescales the KdV equation in terms of dimensionless variables to give only numerical constants.

One can use the Fourier transform to find the solution to (2.1) on the infinite interval $(-\infty < x < \infty)$ for the Cauchy initial value problem, i.e., for $\eta(x, t = 0)$ given, we seek $\eta(x, t)$ for all time t. This may be done by first forming the direct Fourier transform (DFT) of the initial wave $\eta(x, 0)$:

$$F(k) = \int_{-\infty}^{\infty} \eta(x, 0) \exp(-ikx)\, dx. \tag{2.3}$$

The Fourier spectrum changes in time by the simple relation

$$F(k, t) = F(k) \exp(-i\omega t). \tag{2.4}$$

The time evolution of the initial wave is then described by the inverse Fourier transform (IFT):

$$\eta(x, t) = \frac{1}{2\pi} \int_{-\infty}^{\infty} F(k, t) \exp(ikx)\, dk. \tag{2.5}$$

Validity of the Fourier method requires that the usual Dirichlet conditions be satisfied and that

$$\int_{-\infty}^{\infty} |\eta(x, 0)|\, dx < \infty. \tag{2.6}$$

For our own purposes the essential features of the Fourier transform are: (1) The DFT (2.3) generates a wavenumber domain representation of the initial wave which is called the Fourier spectrum; (2) The Fourier spectrum has simple time evolution given by Eq. (2.4); and (3) The IFT (2.5) evolves the initial wave in space and time. Analogs to these three steps are found in the structure of the scattering transform solution to the KdV equation as discussed in the following section.

3. The Scattering Transform Solution to the KdV Equation

The KdV equation describes the motion of small-but-finite amplitude, long waves in shallow water:

$$\eta_t + c_0 \eta_x + \alpha \eta \eta_x + \beta \eta_{xxx} = 0, \qquad -\infty < x < \infty. \tag{3.1}$$

Here $\alpha = 3c_0/2h$; the other variables are defined with respect to (2.1).

The direct scattering problem for a localized nonlinear signal which evolves according to (3.1) is the Schroedinger eigenvalue problem [4]:

$$\psi_{xx} + [\lambda \eta(x, 0) + \kappa^2]\, \psi(x) = 0, \qquad -\infty < x < \infty. \tag{3.2}$$

The constant parameter λ, a measure of nonlinearity to dispersion, is given by $\lambda = \alpha/6\beta$. The solutions to (3.2), with infinite-line boundary conditions, correspond to both real and imaginary wavenumber κ. When the wavenumber takes on some real value $\kappa = k/2$ (division by the arbitrary factor of two ensures that the definition of wavenumber is compatible with that in the Fourier transform (2.3), see Section 4), then the eigensolutions have the following asymptotic boundary conditions:

$$\lim_{x \to -\infty} \psi(x) = a(k) \exp(-ikx/2), \tag{3.3}$$

$$\lim_{x \to \infty} \psi(x) = \exp(-ikx/2) + b(k) \exp(ikx/2). \tag{3.4}$$

The coefficient $b(k)$ in (3.4) is referred to as the *DST continuous spectrum.*

When the wavenumber is imaginary $\kappa = iK_n$ the eigenfunction solutions to (3.2), $\psi_n(x, K_n)$, are bounded only for a finite set of discrete eigenvalues K_n, where

$1 \leqslant n \leqslant N$. Each eigenvalue corresponds to one of the N solitons in the discrete part of the DST spectrum. Each soliton is uniquely related to its amplitude by $\eta_n = 2K_n^2/\lambda$. The remaining part of the discrete spectrum is determined by taking the following normalization for the discrete eigenfunctions:

$$\int_{-\infty}^{\infty} \Psi_n^2(x, K_n)\, dx = 1. \tag{3.5}$$

Associated phase coefficients are then found from

$$C_n = \lim_{x \to \infty} \exp(K_n x)\, \Psi_n(x, K_n). \tag{3.6}$$

The collection of information $\{K_n, C_n, N\}$ is the DST *soliton (discrete) spectrum.* The complete *DST spectrum* is given by the following set of information:

$$\text{DST} = \{K_n, C_n, N; b(k)\}. \tag{3.7}$$

Thus (3.7) is the direct scattering transform of a nonlinear wave evolving by (3.1), just as (2.3) is the direct Fourier transform of a linear wave evolving by (2.1). The connection between the DST and the Fourier transform is discussed in Section 4 below.

The time evolution of the DST spectrum is simple:

$$\begin{aligned} K_n(t) &= K_n, \\ C_n(t) &= C_n \exp(\Omega_n t), \\ N(t) &= N, \\ b(k, t) &= b(k) \exp(-i\omega t). \end{aligned} \tag{3.8}$$

Note the similarity of these equations with the time evolution of the Fourier spectrum (2.4). The linearized dispersion relation for the KdV equation (set $\alpha = 0$ in (3.1) to get (2.1)) can be written in terms of the wavenumber κ of the Schroedinger eigenvalue problem (3.2): $\Omega = \kappa(c_0 - 4\beta\kappa^2)$. Then the dispersion relations for the discrete ($\kappa = iK_n$) and continuous spectra ($\kappa = k/2$) follow:

$$\Omega_n = K_n(c_0 + 4\beta K_n^2), \tag{3.9a}$$

$$\omega = k(c_0 - \beta k^2). \tag{3.9b}$$

These relations are used in (3.8) to evolve the spectrum in time.

The inverse scattering transform (IST) (in analogy with the IFT for linear wave motion) evolves the wave in space and time. We now outline the mathematical structure of IST. One solves the Gelfand–Levitan–Marchenko (GLM) integral equation

$$K(x, y) + B(x + y) + \int_{x}^{\infty} K(x, z)\, B(z + y)\, dz = 0, \qquad y > x, \tag{3.10}$$

whose solution $K(x, y)$ is used to find the wave amplitude for $t \neq 0$:

$$\eta(x, t) = \frac{2}{\lambda} \frac{dK(x, x)}{dx}. \tag{3.11}$$

The kernel of the GLM equation is given by

$$B(r, t) = \sum_{n=1}^{N} C_n^2(t) \exp(-K_n r) + \frac{1}{4\pi} \int_{-\infty}^{\infty} b(k, t) \exp(ikr/2)\, dk. \tag{3.12}$$

We have for convenience suppressed the time dependence in $B(r, t)$ and $K(x, y, t)$ in (3.10) and (3.11). This is possible because the solution to the GLM equation $K(x, y, t)$ (3.10) may be considered to be a function of y only; x and t simply play the role of parameters in the formulation.

The phase coefficients C_n in (3.6) depend upon the normalization (3.5) for the eigenfunction solutions $\psi_n(x, K_n)$ to (3.2). This implies that knowledge of these functions is necessary before the C_n may be found. An alternative expression for the C_n which is independent of the $\psi_n(x, K_n)$ is given by [1, 34]:

$$C_n^2 = -ir_n, \tag{3.13}$$

where the r_n are the residues of the reflection coefficient $b(k)$ at the poles $\kappa = iK_n$:

$$r_n = \frac{1}{2\pi i} \oint b(k)\, dk = i \lim_{K \to K_n} (K - K_n)\, b(iK). \tag{3.14}$$

The right-hand side of this expression obtains because the poles of $b(\kappa)$ are simple. Then the phase coefficients are given by

$$C_n^2 = \lim_{K \to K_n} (K - K_n)\, b(iK). \tag{3.15}$$

Thus the latter expression makes computation of the C_n independent of the $\psi_n(x, K_n)$ and their integrability condition (3.5), a point we exploit in the numerical methods below.

We also note that to compute the number of solitions a convenient formula is [7]:

$$N = \lim_{k \to \infty} [\arg(a(k)) - \arg(a(-k))]. \tag{3.16}$$

This turns out to be a good way to compute N because it too is independent of the eigenfunctions. We discuss the implementation of (3.16) in II.

For the scattering transform to be valid the following integral condition must hold:

$$\int_{-\infty}^{\infty} (1 + |x|)\, |\eta(x, 0)|\, dx < \infty. \tag{3.17}$$

Thus a localized wave field which vanishes rapidly as $|x| \to \infty$ satisfies (3.17). In numerical applications the field $\eta(x, 0)$ is contained in some finite array (i.e., a space series); $\eta(x, 0)$ is assumed to be identically zero outside the confines of this array; hence (3.17) is always satisfied.

In summary, the features of the scattering transform solution to the KdV equation which are of interest in the present context are: (1) The DST (3.2)–(3.6) generates a spectral representation (3.7) of the input wave $\eta(x, 0)$; (2) evolution of the spectrum in time is simple (3.8), (3.9); and (3) the IST (3.10)–(3.12) evolves the wave in time. These three steps are analogous to those for the linear Fourier transform discussed in the last section.

4. The Relationship between the Fourier Transform and the Scattering Transform

Here we briefly discuss the fact that scattering transform theory approaches Fourier transform theory as the wave amplitude becomes small. The inference is that for sufficiently small waves the effect of nonlinearity becomes insignificant and linear Fourier theory is recovered. We emphasize those aspects of the theory which are important to the development of the DST and IST algorithms and to a physical interpretation of the nonlinear wave motion.

The Fourier (small-amplitude) limit occurs in the absence of solitons, i.e., when there are no discrete eigenvalues. A necessary and sufficient condition for no solitons is that $\eta(x, 0)$ be negative definite. We first write the Schroedinger eigenvalue problem (3.2) as an integral equation [35]:

$$\psi(x) = \exp(-ikx/2) - \frac{\lambda}{ik}\int_{-\infty}^{x} \exp(ik\,|x-x'|/2)\,\eta(x', 0)\,\psi(x')\,dx'. \tag{4.1}$$

This expression implicitly contains the boundary conditions (3.3) and (3.4) for the continuous spectrum. To see this we write (4.1) as

$$\psi(x) = \exp(-ikx/2) - \frac{\lambda}{ik}\int_{-\infty}^{x} \exp(ik(x-x')/2)\,\eta(x', 0)\,\psi(x')\,dx'$$

$$-\frac{\lambda}{ik}\int_{x}^{\infty} \exp(ik(x'-x)/2)\,\eta(x', 0)\,\psi(x')\,dx'. \tag{4.2}$$

If we take the limit as $x \to \pm\infty$ we recover (3.3) and (3.4) with explicit expressions for $a(k)$ and $b(k)$ in terms of integrals over the initial wave $\eta(x, 0)$ and eigenfunction $\psi(x)$:

$$a(k) = 1 - \frac{\lambda}{ik}\int_{-\infty}^{\infty} \exp(ikx'/2)\,\eta(x', 0)\,\psi(x')\,dx', \tag{4.3}$$

$$b(k) = -\frac{\lambda}{ik}\int_{-\infty}^{\infty} \exp(-ikx'/2)\,\eta(x', 0)\,\psi(x')\,dx'. \tag{4.4}$$

Thus after solving (3.2) for $\psi(x)$ one can formally obtain $a(k)$ and the continuous DST spectrum $b(k)$ by (4.3) and (4.4). As previously pointed out, however, we shall avoid computation of the eigenfunction $\psi(x)$ (they are not part of the DST spectrum and hence need not be computed) in the numerical methods which follow; simpler means for computing $a(k)$ and $b(k)$ are used instead.

Equations (4.3) and (4.4) are nevertheless useful for establishing the behavior of the DST in the small amplitude limit; the integrals are assumed to be small, so that a Neumann series expansion is possible and we take as a first approximation $\psi^{(0)}(x) \cong \exp(-ikx/2)$, and this, when inserted back into (4.1), gives

$$\psi^{(1)}(x) \cong \exp(-ikx/2) - \frac{\lambda}{ik}\int_{-\infty}^{\infty} \exp(ik\,|x-x'|/2)\,\eta(x',0)\,\psi^{(0)}(x')\,dx', \quad (4.5)$$

a result often referred to as the Born approximation. To this order, approximate expressions for $a(k)$ and $b(k)$ are:

$$a^{(1)}(k) \cong 1 - \frac{\lambda}{ik}\int_{-\infty}^{\infty} \eta(x,0)\,dx, \quad (4.6)$$

$$-ikb^{(1)}(k) \cong \lambda\int_{-\infty}^{\infty} \eta(x,0)\exp(-ikx)\,dx. \quad (4.7)$$

Thus $a^{(1)}(k)$ is related to the area under the initial wave, while $-ikb^{(1)}(k)$ is just the Fourier transform of $\lambda\eta(x,0)$. This establishes the connection between the continuous part of the scattering transform and the Fourier transform. Formally we write for sufficiently small η:

$$-ikb(b) \cong \lambda\int_{-\infty}^{\infty} \eta(x,0)\exp(-ikx)\,dx. \quad (4.8)$$

Note that our use of $\kappa = k/2$ in the Schroedinger eigenvalue problem (3.2) has resulted in a DFT limit (4.8) consistent with the notation used in our definition of the DFT (2.3); this motivates division by a factor of 2 in the wavenumber (3.12).

It is important to establish under what specific conditions we can expect the DST to give results equivalent to the Fourier transform. A crude estimate can be made by letting $\eta(x,0)$ be a square wave centered on the origin, with amplitude η_0 and half-width L, and then (4.6) and (4.7) may be integrated exactly. Given that these integrals must be small for the small amplitude (Born) approximation to be valid, we have

$$\lambda\eta_0/k^2 \ll 1. \quad (4.9)$$

Thus for sufficiently large wavenumber or small amplitude, the DST approaches the Fourier transform. To consider what happens at long wavelength (small k) we note that for some fixed η_0 the Fourier transform limit (4.9) must fail as $k \to 0$. Details of this effect and its physical consequences on shallow water wave motion are

discussed in [26] and cited references. The small amplitude limit condition (4.9) is necessary for demonstrating that the DST numerical algorithm (Section 11) has the Fourier limit for sufficiently small amplitudes (see Section 12).

To obtain additional physical insight we put the condition (4.9) into dimensionless form. In the Schroedinger problem (3.2) we set $\eta(x, 0) = \eta_{\max} u(x)$ and $x = Lr$, where $\eta_{\max}$ is the maximum value of $\eta(x, 0)$ and L is a characteristic length of the initial wave. This gives the dimensionless Schroedinger problem,

$$\psi_{rr} + [\lambda_U u(r) + \chi^2]\psi = 0, \tag{4.10}$$

where $\lambda_U = \lambda \eta_{\max} L^2$ is the Ursell number ([36] and cited references) and $\chi = kL$ is a dimensionless wavenumber. Then condition (4.9) is equivalent to

$$\lambda_U = 3\eta_{\max} L^2/2h^3 \ll \chi^2. \tag{4.11}$$

Thus the Born approximation of quantum mechanics corresponds to small Ursell number in nonlinear, shallow water wave dynamics. Physically, a small Ursell number occurs when nonlinear effects are small; conversely, a large Ursell number corresponds to the case when nonlinear interactions among spectral components are enhanced due to large waves. Note also that (4.9) may be thought of as a *spectral Ursell number*, $\lambda_k = \lambda \eta_0 / k^2$, i.e., an Ursell number associated with each radiation component in the spectrum. Computation of λ_k provides an estimate of how strongly a spectral component interacts with its neighbors: $\lambda_k \ll 1$ for small interactions, $\lambda_k \sim 1$ for moderate interactions, and $\lambda_k \gg 1$ for strong interactions. The linear Fourier transform limit of the DST (4.8) occurs for small spectral Ursell number, $\lambda_k \ll 1$.

We now consider the small amplitude limit of the *inverse scattering transform.* Since no solitons are present, (3.12) can be written:

$$B(2x, t) = \frac{1}{4\pi} \int_{-\infty}^{\infty} b(k) \exp[i(kx - \omega t)]\, dk. \tag{4.12}$$

Segur [37] has shown that the GLM equation may be expanded in a Neumann series for small amplitude waves; the first term in this expansion results from ignoring the integral term of the GLM equation (3.10). With (4.12) this leads to (for small η):

$$\lambda \eta(x, t) \cong \frac{1}{2\pi} \int_{-\infty}^{\infty} [-ikb(k)] \exp[i(kx - \omega t)]\, dk. \tag{4.13}$$

Thus for sufficiently small amplitude the wave motion is recovered at $t = 0$ and is evolved in time thereafter by the inverse Fourier transform. Equation (4.13) is clearly the inverse of (4.8) (compare to (2.3) and (2.5)) and the connection of IST with linear Fourier theory is evident. Note that $F(k) \cong -ikb(k)/\lambda$ in the small amplitude limit. The linear Fourier transform limit (4.13) of the IST (3.10)–(3.12) is seen to occur generally when the spectral Ursell number is small, $\lambda_k \ll 1$.

5. Assumptions Implicit in the Discrete, Finite Fourier Transform

Before proceeding to the development of numerical methods for the DST we first review some of the important considerations which historically lead to discrete algorithms for the Fourier transform. Two of the most important signal processing problems relate to the use of *Fourier series* (for signals periodic on an interval $(0, L)$) and the *Fourier transform* (for nonperiodic signals on the infinite interval). The theoretical properties of Fourier series and Fourier transforms differ somewhat, but, fortunately for most practical problems in data analysis, their digital computational procedures are normally the same [2]. This results from the fact that only a finite range Fourier series or transform can be computed from digital signals and normally this finite range is taken to be the period of an associated Fourier series. The above observation ultimately motivated the detailed study of *periodic nonlinear Fourier analysis* [22–30, 38–42].

We are thus led to a discussion of the finite Fourier transform. We first restrict the limits of (2.3) to a finite spatial interval $(0, L)$ on which there lies a localized initial wave $\eta(x, 0)$ which is taken to be zero outside this interval:

$$F(k) = \int_0^L \eta(x, 0) \exp(-ikx)\, dx. \tag{5.1}$$

We further assume that $\eta(x, 0)$ is sampled at M equally spaced values of x a distance Δx $(= L/M)$ apart so that $x_m = m\,\Delta x$ and

$$\eta_m = \eta(m\,\Delta x, 0), \qquad m = 0, 1, 2, \ldots, M-1. \tag{5.2}$$

For arbitrary wavenumber k the discrete version (rectangular approximation) of (5.1) is

$$F(k) = \Delta x \sum_{m=0}^{M-1} \eta_m \exp(-ikx_m). \tag{5.3}$$

One then selects discrete wavenumbers for evaluation of $F(k)$:

$$k_j = j\,\Delta k = \frac{2j\pi}{L} = \frac{2j\pi}{M\,\Delta x}, \qquad j = 0, 1, 2, \ldots, M-1. \tag{5.4}$$

The Fourier components are then found from

$$F(k_j) = \Delta x \sum_{m=0}^{M-1} \eta_m \exp(-ik_j x_m) = \frac{L}{M} \sum_{m=0}^{M-1} \eta_m \exp[-2\pi i(jm/M)], \tag{5.5}$$

where $\Delta k = 2\pi/L$. The right-hand side of (5.5) is often referred to as the definition of the discrete, finite Fourier transform whose mathematical properties have been studied in detail [3]. The components of $F(k_j)$ are unique only out to the Nyquist frequency which occurs for $j = M/2$.

The easiest way to evaluate (5.3) or (5.5) numerically is through the simple recursion relation

$$F_m(k) = F_{m-1}(k) + \eta_m z^{-mk} \Delta x, \tag{5.6}$$

where $F_{-1}(k) = 0$ and $z = \exp(i \Delta x)$. It is clear that such an algorithm requires M^2 operations (ranging over both space x and wavenumber k), where an operation is defined as "multiplication of an exponential times an amplitude, followed by a summation." Fast Fourier transform (FFT) techniques allow the $F(k_j)$ to be computed by an algorithm equivalent to (5.5), (5.6) but which requires only $M(\log M)$ operations. Herein we develop an algorithm for the direct scattering transform which is analogous to (5.6), i.e., two-point recursive. Development of this DST algorithm, however, is not as simple or obvious as the step from (5.3) or (5.5) to (5.6) for the Fourier transform. A "fast" DST algorithm must await future developments. Nevertheless it is important to note that we are seeking a numerical algorithm which has discrete Fourier structure.

Some points are worth noting about the assumptions implicit in the above procedures. First, in the context of numerical analysis (as opposed to data analysis), note that while the rectangular approximation was used for evaluation of the integral (5.1), corrections to (5.1) for trapezoidal and higher order approcimations can be made if desired (for a discussion and references see Ng [43]). The usual procedure in signal processing applications, however, is to employ the FFT algorithm (based upon (5.5) which is equivalent to the two-point recursive formula (5.6)) for the spectral analysis of data and of other (say computer generated) digital signals [2, 3]. No corrections are normally considered at higher order, primarily because of ignorance about the behavior of the signal at intermediate locations between the discrete points. In the analysis of data one normally measures a time series of several thousand points with a small discretization interval (in either time or space) and this implies that higher order corrections are likely not very significant.

An important consideration about the infinite-interval Fourier transform $F(k)$ relates to how the wavenumbers are selected for numerical computation. Based upon known results for the periodic Fourier transform, a convenient wavenumber resolution is (see (5.4))

$$\Delta k = 2\pi/L, \tag{5.7}$$

where L is the period. The upper frequency cutoff is given by the Nyquist wavenumber

$$k_N = \pi/\Delta x. \tag{5.8}$$

Theoretically one assumes knowledge of the wave amplitude over the entire (infinite) real axis. This implies that knowledge of all wavenumbers are necessary to reconstruct the wave. In numerical computation of the *infinite-interval Cauchy problem* one normally measures or generates a discrete signal which is appreciably different from zero only on some interval $(0, L)$ and which is *assumed* to be zero

everywhere outside this interval. The implication is that the signal has infinite length and according to (5.7) we have $\Delta k \to 0$. Thus the wavenumber k is essentially continuous, a known result of Fourier transform theory. What this means in a practical sense is that while (5.7) forms some basis for resolving the wavenumbers, one can deviate from this and use a smaller wavenumber resolution in the spectrum if desired. The Nyquist cutoff given by (5.8) must also be selected with care. One must use a sufficiently small Δx to ensure that the interval $(0, k_N)$ contains most of the spectral energy. Otherwise aliasing of spectral components may occur just as in linear Fourier analysis. Furthermore, one must keep in mind that the finite Fourier transform (5.5) is a periodic algorithm; the true infinite-line Cauchy problem is approached only as $L \to \infty$.

6. Toward a Discrete Algorithm for the Direct Scattering Transform

In the previous section we saw that the assumptions leading to the discrete, finite Fourier transform include: (1) truncation of a localized discrete signal to some finite interval $(0, L)$ and (2) rectangular approximation of the Fourier integral. These result in (5.3) and, with an appropriate selection for the wavenumbers, one finds (5.5), which is the finite Fourier transform. In order to develop a numerical algorithm for the DST we shall consider (5.3) as fundamental (thus deferring selection of the wavenumbers to a later section) and proceed to find an algorithm which approaches (5.3) when the wave amplitude becomes sufficiently small. Thus (5.3) is an important guiding criterion in what follows. In this way we develop nonlinear spectral methods which are compatible with known discrete Fourier methods.

In order to pursue an algorithm for the direct scattering transform we consider, as before, a discrete signal with amplitudes at coordinate positions $x_m = m\,\Delta x$, where Δx is a constant spatial interval between points and $0 \leqslant m \leqslant M-1$ (we could also generalize the results to a finite element analysis in which Δx is not constant, but we do not pursue this here since Δx is normally constant for measured data and for computer generated space or time series). In order to truncate the signal to some interval $(0, L) = (0, (M-1)\,\Delta x)$ we assume that all wave amplitudes are zero to the left of and including x_0 and to the right of and including x_M. Recall that the rectangular approximation (5.3) for the Fourier integral (5.1) implies $\eta(x, 0)\exp(-ikx)$ is a (complex) constant in each interval Δx. Since this product of amplitude and exponential do not appear explicitly in the Schroedinger eigenvalue problem it does not appear straightforward to use the same form of rectangular approximation here.

However, we have been able to develop an alternate discretization which, for practical purposes, works rather well (see Fig. 1). A continuous wave amplitude function $\eta(x, 0)$ (Fig. 1a) is discretized at intervals $x_m = m\,\Delta x(\eta(x_m, 0)$, Fig. 1b). The discrete signal is then replaced by a piecewise constant function as shown in Fig. 1c. Each constant partition has width Δx centered on coordinate x_m; the con-

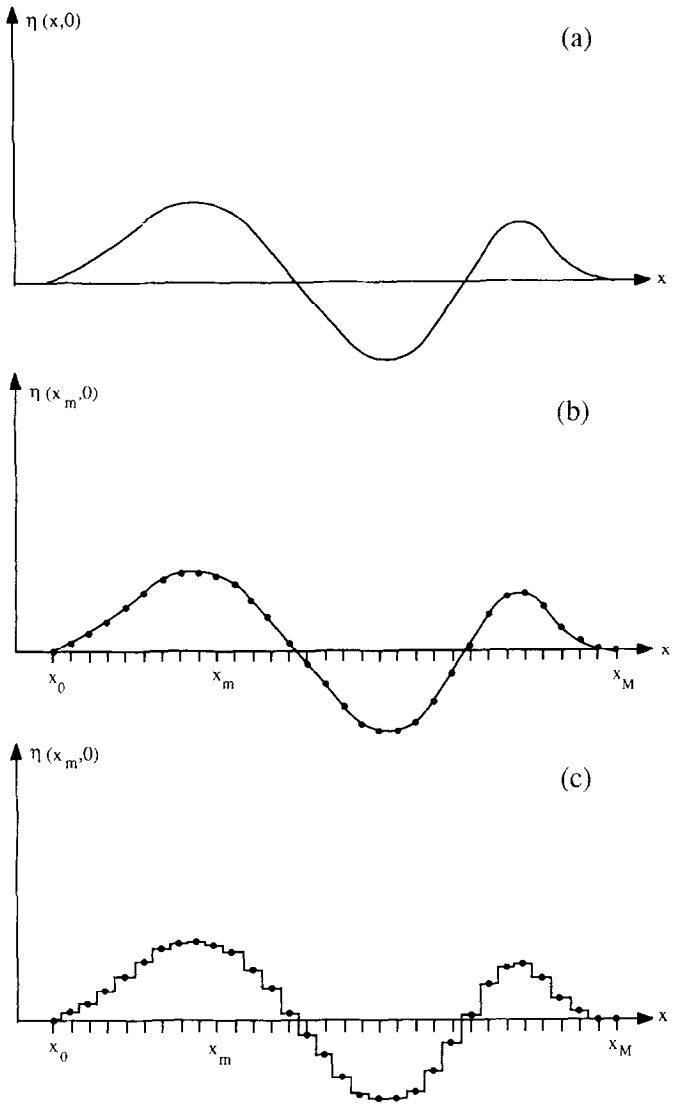

FIG. 1. An initial wave amplitude function $\eta(x, 0)$ which varies continuously as a function of x is shown in (a) and is discretized at intervals Δx in (b). In (c) one associates a piecewise constant function with the discrete array (b). This latter function (c) is then used in the development of the numerical algorithm for the direct scattering transform (DST).

stant amplitude η_m in each interval is assumed to be the same as the amplitudes of the previous discretization procedure for the Fourier transform. In selecting this form for the wave amplitude function we are also motivated by the fact that the Schroedinger eigenvalue problem has an exact solution for functions of this type.

Since we consider a signal of this kind to be almost as good as the original rectangular approximation to (5.1) we would like to compare the Fourier transform of the two types of wave forms. For the piecewise constant signal one easily finds for the Fourier integral

$$F_p(k) = \Delta x \left[\frac{\sin(k\,\Delta x/2)}{(k\,\Delta x/2)} \right] \sum_{m=0}^{M-1} \eta_m \exp(-ikx_m), \tag{6.1}$$

a result which is amazingly close to (5.3), differing only by the factor in square brackets. This factor acts essentially as a filter which relates the Fourier spectrum $F(k)$ (5.3) for a *discrete signal* to the Fourier transform $F_p(k)$ (6.1) for a *piecewise constant signal.* We set

$$S(k\,\Delta x) = \frac{\sin(k\,\Delta x/2)}{(k\,\Delta x/2)}. \tag{6.2}$$

A graph of this function is shown in Fig. 2. For $k\,\Delta x$ sufficiently small $S(k\,\Delta x) \cong 1$, and we have $F_p(k) \cong F(k)$. Thus the Fourier transform for the discrete and piecewise constant signals are essentially equal for sufficiently small wavenumber. The filter $S(k\,\Delta x)$ slowly and monotonically decreases towards its first zero at $k_0 = 2\pi/\Delta x$. The Nyquist wavenumber occurs at half this value $k_N = k_0/2 = \pi/\Delta x$, where $S(k\,\Delta x)$ has decreased to 0.64.

It is important at this point to understand what influence the filter (6.2) may have on the physics of the DST spectrum (as derived below in Sections 8–11). In

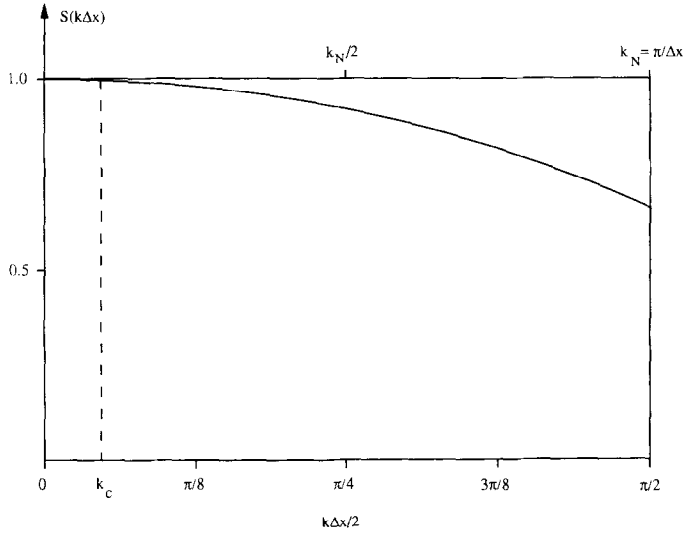

FIG. 2. Shape of the filter which relates the direct Fourier transform (DFT) of a discrete function to the DFT of a piecewise constant function.

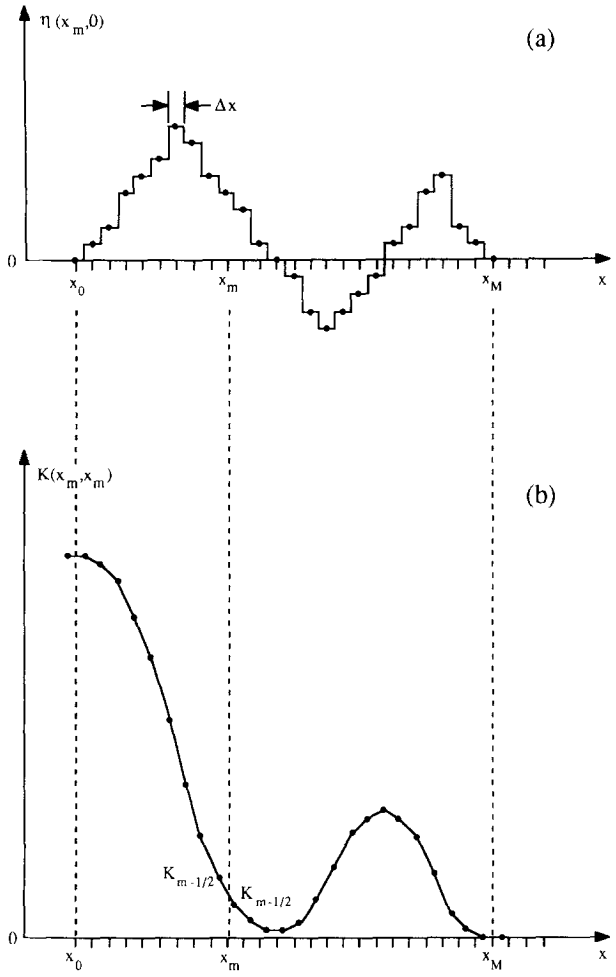

FIG. 3. A piecewise constant wave amplitude function $\eta(x_m, 0)$ (a) corresponds to a piecewise linear solution to the Gelfand–Levitan–Marchenko integral equation (b).

problems of water wave motion a wavenumber cutoff beyond which KdV evolution does not apply is given approximately by $k_c = 1/h$. (The is because the long wave assumption is no longer valid for larger wavenumbers much greater that k_c.) Normally $k_c/k_N \sim 0.01$–0.1 [26] and for $k \gg k_c$ the DST spectrum approaches the Fourier transform. Thus in the wavenumber range in which KdV physics is important $(0, k_c)$ one can normally arrange for $S(k\,\Delta x)$ to be near one (by making Δx sufficiently small so that $S(k\,\Delta x) \cong 1$) and one need not be concerned with the presence of the filter. One can always remove the filter from the spectrum by dividing the continuous DST spectrum by (6.2) if a direct comparison with the FFT is desired. This latter procedure is recommended in practical implementations of the

algorithm (see II). Another important point is that since the filter differs from 1 only at high wavenumbers (if the Nyquist wavenumber is chosen large enough), where the physics is essentially linear, it is unlikely that nonlinear effects can strongly influence the actual shape of the filter for the DST spectrum.

Another additional concern is to establish what effect the selection of a piecewise constant wave form has on the algorithm for the *inverse scattering transform*, i.e., for the selection of a numerical method for the solution of the GLM equation (3.10). The relationship between the solutions of GLM, $K(x, x)$, and the solution of KdV, $\eta(x, 0)$ can be seen by rewriting (3.11) as

$$K(x, x) = -\frac{\lambda}{2}\int_x^\infty \eta(x, 0)\, dx. \tag{6.3}$$

We write the discrete (piecewise constant) form for (6.3):

$$K_{m+1/2} = -\frac{\lambda}{2}\Delta x \sum_{j=m}^{M} \eta_{j+1}. \tag{6.4}$$

This implies that in order to be consistent with our selection of a piecewise constant wave, the solution of the GLM equation must be trapezoidal as shown in Fig. 3b. $K(x, x)$ is a piecewise linear fuction evaluated at the positions $x_{m+1/2}$, i.e., at the half-integers $m+\frac{1}{2} = \frac{1}{2}, \frac{3}{2}, \frac{5}{2}, \ldots, M+\frac{1}{2}$. The initial (piecewise constant) wave may be recovered by the obvious discrete formula (see Fig. 3):

$$\eta_m = \frac{2}{\lambda}\frac{(K_{m+1/2} - K_{m-1/2})}{\Delta x}. \tag{6.5}$$

Thus our discretization procedure for the DST (developed by analogy with Fourier analysis) has led to the need for an IST procedure which is trapezoidal. A trapezoidal algorithm for solving the GLM equation has been given by Hald [44]. Paper III discusses implementation of the GLM algorithm for nonlinear filter applications and for evolving wave motion forward or backward in time.

7. Searching for a DST Numerical Algorithm from Available Numerical Methods

In this section we briefly survey existing numerical methods for solving the Schroedinger eigenvalue problem. Even though, to our knowledge, no one else has attempted to solve this problem in the context of Fourier analysis, we originally anticipated no great difficulty in adapting the work of others in the present context. Thus our original hope was to discover some previously developed algorithm(s) which would satisfy the guiding criteria set forth in the previous section. To this end we now briefly review four frequently used techniques for numerically integrating the Schroedinger equation.

(1) "Shooting" or step-by-step methods. These are based on the finite-difference scheme in which the second derivative of the eigenfunction at some point x is approximated from values of the eigenfunction at x, $x \pm \Delta x$, $x \pm 2\,\Delta x$, etc. One uses a numerical integrator and "shoots" the eigenfunction from one boundary to the other for a given value of the wavenumber κ. The value of κ is varied so as to fulfill the boundary condition at the second boundary. Useful references for this method are [45–51].

(2) Finite-element methods. One divides the domain into regions where the amplitude function (a "potential") does not change rapidly. Then one replaces the amplitude function by a piecewise constant (or piecewise linear or quadratic) function. In each partition the eigenfunction is then exponential (or described by Airy functions for a piecewise linear or parabolic cylinder functions for a piecewise quadratic eigenfunction). Then one ensures continuity of the eigenfunction and its first derivative between partitions and finally one satisfies the boundary conditions to obtain the solution [52–55].

(3) The spectral [54] or Rayleigh–Ritz–Galerkin [56] method. One expands the eigenfunctions in some basis which may or may not be orthogonal and one seeks the solution of the associated secular equation. The basis is normally selected so that the matrix elements are easy to compute, for example, by sines [57], splines [58], or Gaussians [59]. Other useful references are [60–63].

(4) Global matrix methods. The finite-difference methods can be expressed in matrix (or global) form [60, 64–66]. Normally only a few off-diagonal terms are taken; Padé approximants have been used to generalize the techniques to a larger number of off-diagonal terms [67]. A more thorough review of numerical methods for solving the Schroedinger eigenvalue problem is given in [67].

In an attempt to adapt some of the above available methods to our own use first note that the last section specifies that the wave amplitude $\eta(x, 0)$ should preferably be treated as piecewise constant. We have therefore considered available methods in the finite-element class above as discussed in Refs. [52–55]. Unfortunately we have not been very successful in carrying over the methods to our present application. We were unable to discover how to make these methods conform to many of the requirements of Section 6. We note that the paper by Canosa and Oliveira [52] comes closest to the spirit of what we are trying to accomplish: integration of the Schroedinger equation for a piecewise constant potential. Our formulation, guided by our requirements based upon nonlinear Fourier analysis, bears little resemblance to theirs, however. As far as we know the restrictions listed in Section 6 have not heretofore been placed upon the development of an algorithm for solving the Schroedinger eigenvalue problem. Because many of the requirements have not been addressed or satisfied in the literature, and because we were unable to discover how to modify available algorithms to suit our needs, we concluded that a search for a new algorithm might be appropriate. This led to the development of the methods

described herein (which we call Fourier signal processing methods) as opposed to those methods most often cited in the literature (numerical analysis methods). The results of our research in this regard are given in the following sections.

8. The DST of a Rectangular Initial Wave

Our goal is to seek the solution to the Schroedinger eigenvalue problem for a piecewise constant wave amplitude function $\eta(x, 0)$ (see Figs. 1, 3). To this end we first obtain the solution for a rectangular initial wave, the "particle in a box" problem, which is treated in standard quantum mechanics texts [68, 69]. Here we review these methods from the standpoint of nonlinear spectral analysis in terms of the *transfer* or *spectral* matrix of the theory. This step is essential (1) for understanding the details of the nonlinear Fourier approach, (2) for establishing the notation, (3) for extending the method to the more general case for $\eta(x, 0)$ piecewise constant, (4) for making the connection between quantum mechanics and long wave hydrodynamics, (5) for extending the approach to the periodic problem [27–30], and (6) for rigorous checkout of the numerical algorithm (see II). We take $\eta(x, 0)$ to be a single rectangular initial wave pulse centered on the origin:

$$\begin{aligned} \eta(x, 0) &= \eta_0, \qquad |x| \leqslant a; \\ &= 0, \qquad |x| > a. \end{aligned} \tag{8.1}$$

The solution to the Schroedinger eigenvalue problem is given by

$$\psi(x) = \begin{cases} A\exp(i\kappa x) + B\exp(-i\kappa x); & x < -a \\ C\exp(i\zeta x) + D\exp(-i\zeta x); & -a \leqslant x \leqslant a \\ E\exp(i\kappa x) + F\exp(-i\kappa x); & x > a \end{cases} \tag{8.2}$$

where A–F are complex constants depending upon the wavenumber κ; also

$$\zeta = (\lambda\eta_0 + \kappa^2)^{1/2}. \tag{8.3}$$

$\psi(x)$ and $\psi_x(x)$ are continuous at both $x = \pm a$, so that matrices may be computed between coefficient pairs of (8.2):

$$\begin{pmatrix} A \\ B \end{pmatrix} = \mathbf{T}_1(\kappa)\begin{pmatrix} C \\ D \end{pmatrix}, \qquad \begin{pmatrix} C \\ D \end{pmatrix} = \mathbf{T}_2(\kappa)\begin{pmatrix} E \\ F \end{pmatrix}. \tag{8.4}$$

The matrices $\mathbf{T}_1(\kappa)$ and $\mathbf{T}_2(\kappa)$ are given by

$$\mathbf{T}_1(\kappa) = \frac{1}{2}\begin{pmatrix} (1+\zeta/\kappa)\exp[i(\kappa-\zeta)a] & (1-\zeta/\kappa)\exp[i(\kappa+\zeta)a] \\ \end{pmatrix} \tag{8.5}$$

$$\mathbf{T}_2(\kappa) = \frac{1}{2}\begin{pmatrix} (1+\kappa/\zeta)\exp[i(\kappa-\zeta)a] & (1-\kappa/\zeta)\exp[-i(\kappa+\zeta)a] \\ (1-\kappa/\zeta)\exp[i(\kappa+\zeta)a] & (1+\kappa/\zeta)\exp[-i(\kappa-\zeta)a] \end{pmatrix}. \tag{8.6}$$

Thus

$$\begin{pmatrix} A \\ B \end{pmatrix} = \mathbf{M}(\kappa) \begin{pmatrix} E \\ F \end{pmatrix}; \qquad \mathbf{M}(\kappa) = \mathbf{T}_1(\kappa)\,\mathbf{T}_2(\kappa), \tag{8.7}$$

where

$$\mathbf{M}(\kappa) = \begin{pmatrix} [\cos 2\zeta a - i\delta \sin 2\zeta a] \exp(2i\kappa a) & -i\gamma \sin 2\zeta a \\ i\gamma \sin 2\zeta a & [\cos 2\zeta a + i\delta \sin 2\zeta a] \exp(-2i\kappa a) \end{pmatrix} \tag{8.8}$$

$$\text{with } \gamma = \frac{1}{2}\left(\frac{\zeta}{\kappa} - \frac{\kappa}{\zeta}\right); \qquad \delta = \frac{1}{2}\left(\frac{\zeta}{\kappa} + \frac{\kappa}{\zeta}\right). \tag{8.9}$$

Note that $\det \mathbf{M} = M_{11}M_{22} - M_{12}M_{21} = 1$ and that for real wavenumber $\kappa = k/2$, $M_{22} = M_{11}^*$, $M_{21} = M_{12}^*$. The matrix $\mathbf{M}(\kappa)$ (8.8) plus boundary conditions (3.3), (3.4), and (3.6) entirely describe the solution to the spectral eigenvalue problem (3.2). This formulation provides an immediate and direct means for obtaining the DST of the square pulse (8.1) as we now discuss.

In order to compute the continuous part of the DST spectrum we set $\kappa = k/2$ and use the boundary conditions (3.3), (3.4), in (8.7):

$$\begin{pmatrix} 0 \\ a(k) \end{pmatrix} = \mathbf{M}(\kappa = k/2) \begin{pmatrix} b(k) \\ 1 \end{pmatrix}. \tag{8.10}$$

This leads to simple expressions for the coefficients $a(k)$ and $b(k)$ in terms of the matrix elements of $\mathbf{M} = \mathbf{M}(k/2)$:

$$a(k) = \frac{1}{M_{11}(k/2)} = \frac{\exp(-ika)}{(\cos 2\zeta a - i\delta \sin 2\zeta a)}, \tag{8.11}$$

$$b(k) = -\frac{M_{12}(k/2)}{M_{11}(k/2)} = i\gamma a(k) \sin 2\zeta a, \tag{8.12}$$

where we have used the fact that $\det \mathbf{M} = 1$. Thus, after computing the matrix $\mathbf{M} = \mathbf{M}(k/2)$ the continuous part of the spectral transform $b(k)$ easily follows.

For the discrete spectrum we use (3.6) in (8.7) and set $\kappa = iK_n$ to find

$$\begin{pmatrix} 0 \\ D_n \end{pmatrix} = \mathbf{M}(\kappa = iK_n) \begin{pmatrix} C_n \\ 0 \end{pmatrix}. \tag{8.13}$$

The constant D_n arises because we take

$$\lim_{x \to -\infty} \psi_n(x, K_n) = D_n \exp(K_n x).$$

Equation (8.13) is satisfied at the eigenwavenumbers K_n (or soliton amplitudes $\eta_n = 2K_n/\lambda$). Thus the zeros of

$$M_{11}(iK_n) = 2K_n\zeta_n - (\zeta_n^2 - K_n^2) \tan 2\zeta_n a = 0, \tag{8.14}$$

or the poles of $b(iK_n) = -M_{12}(iK_n)/M_{11}(iK_n)$, give the eigenvalues K_n. Equation (8.13), together with (3.5), can be solved for the normalization coefficients C_n, D_n. Their ratio may be found from

$$\frac{C_n}{D_n} = -M_{12}(iK_n) = i\gamma_n \sin 2\zeta_n a = \pm 1, \tag{8.15}$$

The added constraint (3.5) must be imposed in order to fix the constant D_n. In the present case $C_n = \pm D_n$ because the symmetric rectangular pulse has been centered about the origin; for the plus sign the eigenfunction solution $\psi_n(x, K_n)$ is an even function, while for the negative sign it is an odd function.

Phase coefficients independent of the eigenfunctions $\psi_n(x, K_n)$ may be found from (3.15) and (8.12):

$$C_n^2 = \lim_{K \to K_n} (K - K_n) \frac{\gamma_0 \sin 2\zeta a \exp(Ka)}{(\cos 2\zeta a + \delta_0 \sin 2\zeta a)}, \tag{8.16}$$

where

$$\begin{aligned} \zeta &= (\lambda\eta_0 - K^2)^{1/2}, \\ \gamma_0 &= \frac{1}{2}\left(\frac{K}{\zeta} + \frac{\zeta}{K}\right), \\ \delta_0 &= \frac{1}{2}\left(\frac{K}{\zeta} - \frac{\zeta}{K}\right). \end{aligned} \tag{8.17}$$

Thus the eigenvalues K_n are found numerically from (8.14) and the C_n are found by numerical solution of (8.16) and (8.17).

The number of solitions is likewise easy to find:

$$N = \frac{2(\lambda\eta_0)^{1/2} a}{\pi} + 1. \tag{8.18}$$

For the above simple case of an initial rectangular wave pulse the DST has been reduced to computing the matrix $\mathbf{M}$ (which is often called the *transfer matrix*, but which we prefer to call the *spectral matrix* in the present application) as given by (8.8) and, subsequently, using (8.14), (8.16), and (8.18) to compute the discrete spectrum and (8.12) to compute the continuous spectrum. Note that we place special emphasis on the spectral matrix $\mathbf{M}(\kappa)$; given this matrix the DST spectrum easily follows. The emphasis remains on this matrix in the numerical model described below. This formulation has the added advantage that the spectral matrix is easily related to the *monodromy matrix* of periodic KdV theory [27, 28, 32, 38]; extension of our algorithm to the periodic scattering transform is thus straightforward.

9. The DST of a Piecewise Constant Initial Wave

To generalize the results of the last section to an initial pulse or packet of arbitrary shape (see Fig. 3a) we assume that the continuous function $\eta(x, 0)$ can be discretized into M values at intervals Δx in the spatial variable x as shown in Fig. 3b; this gives discrete amplitudes $\{\eta_m\}$ at coordinate values $\{x_m\}$. We then associate with this discrete array the piecewise constant, discontinuous function (shown in Fig. 1c) defined by

$$\begin{aligned} \eta(x, 0) &= \eta_m, \qquad x_{m-1/2} \leqslant x \leqslant x_{m+1/2} \\ &= 0, \qquad x \leqslant x_1, x \geqslant x_{M-1}, \end{aligned} \tag{9.1}$$

where we have assumed that $\eta(x, 0) = 0$ outside (x_0, x_M) for consistency with the localization condition (3.17); note for later convenience that we also take $\eta_0 = \eta_1 = \eta_{M-1} = \eta_M = 0$ and that

$$x_m = m\,\Delta x. \tag{9.2}$$

Based upon considerations discussed in the last section, the spectral matrix $M(\kappa)$ for the function (9.1) is given by

$$\mathbf{M}(\kappa) = \prod_{m=0}^{M} \mathbf{T}_m(x'_m, \zeta_m, \zeta_{m+1}), \tag{9.3}$$

where the matrix $\mathbf{T}_m$ has the form

$$\begin{aligned} &\mathbf{T}_m(x'_m, \zeta_m, \zeta_{m+1}) \\ &= \frac{1}{2}\begin{pmatrix} (1+\zeta_{m+1}/\zeta_m)\exp[i(\zeta_{m+1}-\zeta_m)x'_m] & (1-\zeta_{m+1}/\zeta_m)\exp[-i(\zeta_{m+1}+\zeta_m)x'_m] \\ (1-\zeta_{m+1}/\zeta_m)\exp[i(\zeta_{m+1}+\zeta_m)x'_m] & (1+\zeta_{m+1}/\zeta_m)\exp[-i(\zeta_{m+1}-\zeta_m)x'_m] \end{pmatrix} \end{aligned} \tag{9.4}$$

and

$$\zeta_m = [\lambda\eta_m + \kappa^2]^{1/2}, \tag{9.5}$$

$$x'_m = x_m + \Delta x/2. \tag{9.6}$$

The matrix $\mathbf{M}$ has unit determinant and for real wavenumber $\kappa = k/2$, $M_{22} = M_{11}^*$, and $M_{21} = M_{12}^*$. Note that the integer m ranges over the number of discrete points in the initial wave pulse, $0 \leqslant m \leqslant M$. The integer m is not to be confused with the integer n which ranges over $1 \leqslant n \leqslant N$, where N is the number of solitons.

Given the matrix $\mathbf{M}(k)$ (9.3), (9.4) we can compute the continuous spectrum $b(k)$ in analogy with (8.12) by setting $\kappa = k/2$:

$$b(k) = -\frac{M_{12}(k/2)}{M_{11}(k/2)}. \tag{9.7}$$

The wavenumber k is, of course, continuous in the range $(-\infty < k < \infty)$, where $b(-k) = b^*(k)$. The procedure which we use to select the wavenumbers at which (9.7) is to be evaluated follows (5.4); a discussion is found in II.

To find the discrete spectrum we use $\kappa = iK_n$ and search the range $0 \leqslant \eta_n (= 2K_n^2/\lambda) \leqslant 2\eta_{\max}$, where $\eta_{\max}$ is the maximum value of the amplitudes $\{\eta_m\}$. The eigenvalues are the zeros of (recall (8.14)):

$$M_{11}(iK_n) = 0. \tag{9.8}$$

Then the phase coefficients are computed as the residues of the reflection coefficient (which correspond to the discrete eigenvalues):

$$C_n^2 = \lim_{K \to K_n} (K - K_n)\, b(iK). \tag{9.9}$$

The number of solitons may be computed from the transmission coefficient $a(k)$ [7]:

$$N = \lim_{k \to \infty} \{\arg[a(k)] - \arg[a(-k)]\}, \tag{9.10}$$

where as before (8.11),

$$a(k) = \frac{1}{M_{11}(k/2)}. \tag{9.11}$$

This completes our discussion of the exact solution to the Schroedinger eigenvalue problem (and the associated exact form of the DST spectrum) for a piecewise continuous initial wave.

10. Factorization of the Spectral Matrix into $SU(2)$ Rotations; A Well-Behaved Form for the DST Algorithm

While Eqs. (9.3)–(9.11) give the exact solution to the Schroedinger problem for a discrete wave (9.1), they do not turn out to be very useful for computational purposes. The reason for this unfortunate circumstance is due to "exploding exponentials" which may occur during the search for the discrete eigenvalues. This results in large roundoff errors and in numbers which may exceed the range of most computers. These difficulties can be alleviated however by noting that the $\mathbf{T}_m$ matrix may be factored as

$$\mathbf{T}_m = \left(\frac{\zeta_{m+1}}{\zeta_m}\right)^{1/2} \mathbf{Q}_m \mathbf{R}_m \mathbf{S}_m, \tag{10.1}$$

where the matrices $\mathbf{Q}_m$, $\mathbf{R}_m$, and $\mathbf{S}_m$ are $SU(2)$ rotations and are given by

$$\mathbf{Q}_m = \begin{pmatrix} \exp(-i\zeta_m x'_m) & 0 \\ 0 & \exp(i\zeta_m x'_m) \end{pmatrix} \tag{10.2}$$

$$\mathbf{R}_m = \begin{pmatrix} \cos(\theta_m/2) & i\sin(\theta_m/2) \\ i\sin(\theta_m/2) & \cos(\theta_m/2) \end{pmatrix} \tag{10.3}$$

$$\mathbf{S}_m = \begin{pmatrix} \exp(i\zeta_{m+1} x'_m) & 0 \\ 0 & \exp(-i\zeta_{m+1} x'_m) \end{pmatrix}, \tag{10.4}$$

where

$$\cos(\theta_m/2) = \frac{(\zeta_m + \zeta_{m+1})}{2(\zeta_m \zeta_{m+1})^{1/2}} \tag{10.5}$$

$$i\sin(\theta_m/2) = \frac{(\zeta_{m+1} - \zeta_m)}{2(\zeta_m \zeta_{m+1})^{1/2}}. \tag{10.6}$$

Here ζ_m is given by (9.5).

If the factored form for the $\mathbf{T}_m$ matrix is inserted back into the expression for the spectral matrix (9.3), we find, after collecting matrix elements as a function of $\Delta x = x_{m+1} - x_m$,

$$\mathbf{M} = \mathbf{B}\mathbf{M}'\mathbf{A}, \tag{10.7}$$

where

$$\mathbf{M}' = \prod_{m=1}^{M-1} \Delta\mathbf{T}_m, \tag{10.8}$$

$$\mathbf{B} = \begin{pmatrix} \exp[-i\kappa(x_0 + \Delta x/2)] & 0 \\ 0 & \exp[i\kappa(x_0 + \Delta x/2)] \end{pmatrix}, \tag{10.9}$$

and

$$\mathbf{A} = \begin{pmatrix} \exp[i\kappa(x_M - \Delta x/2)] & 0 \\ 0 & \exp[-i\kappa(x_M - \Delta x/2)] \end{pmatrix}. \tag{10.10}$$

In (10.8) we have the "delta $\mathbf{T}_m$" matrix, $\Delta\mathbf{T}_m$, which is a function of Δx rather than x_m and is given by

$$\Delta\mathbf{T}_m = \begin{pmatrix} \dfrac{(\zeta_m + \zeta_{m+1})}{2\zeta_m} \exp(-i\zeta_m \Delta x) & \dfrac{(\zeta_m - \zeta_{m+1})}{2\zeta_m} \exp(-i\zeta_m \Delta x) \\ \dfrac{(\zeta_m - \zeta_{m+1})}{2\zeta_m} \exp(i\zeta_m \Delta x) & \dfrac{(\zeta_m + \zeta_{m+1})}{2\zeta_m} \exp(i\zeta_m \Delta x) \end{pmatrix}. \tag{10.11}$$

Note that the terms $(\zeta_{m+1}/\zeta_m)^{1/2}$ in (10.1) have canceled out in the computation of (10.11).

Eqs. (9.3)–(9.6) are equivalent to (10.7)–(10.11); thus the latter equations also give the exact solution to the Schroedinger problem for a piecewise constant wave form. However, the latter formulation is a function of Δx rather than x_m. Thus the problem of exploding exponentials is much reduced because Δx is typically a rather small number compared to x_m, which ranges up to the length of the discrete initial wave. Furthermore, roundoff error is also reduced because each of the $\Delta \mathbf{T}_m$ matrices is $O(1)$. Another advantage of this formulation is that recursion relations exist for the $\mathbf{M}'$ matrix. These relations, which we discuss in the next section, lead to a significant increase in the speed of the DST algorithm.

11. Recursion Relations for the DST Algorithm

To develop recursion relations for the $\mathbf{M}$ matrix we rewrite (10.11) as

$$\Delta \mathbf{T}_m = \begin{pmatrix} s_m z^{-\zeta_m} & d_m z^{-\zeta_m} \\ d_m z^{\zeta_m} & s_m z^{\zeta_m} \end{pmatrix}, \tag{11.1}$$

where

$$z = \exp(i\,\Delta x) \tag{11.2}$$

$$d_m = \frac{(\zeta_m - \zeta_{m+1})}{2\zeta_m} \tag{11.3}$$

$$s_m = \frac{(\zeta_m + \zeta_{m+1})}{2\zeta_m}. \tag{11.4}$$

With a little work we find that the matrix $\mathbf{M}'$ may then be written

$$\mathbf{M}' = \prod_{m=1}^{M-1} \Delta \mathbf{T}_m = \begin{pmatrix} z^{-\rho_{M-1}} F_{M-1}(z) & z^{-\rho_{M-1}} G_{M-1}(z) \\ z^{\rho_{M-1}} G_{M-1}(1/z) & z^{\rho_{M-1}} F_{M-1}(1/z) \end{pmatrix}, \tag{11.5}$$

such that $F_m(z)$ and $G_m(z)$ satisfy the recursion relations

$$\begin{pmatrix} F_m(z) \\ G_m(z) \end{pmatrix} = \begin{pmatrix} s_m & d_m z^{2\zeta_m} \\ d_m & s_m z^{2\zeta_m} \end{pmatrix} \begin{pmatrix} F_{m-1}(z) \\ G_{m-1}(z) \end{pmatrix} \tag{11.6}$$

with

$$F_0(z) = 1, \qquad G_0(z) = 0 \tag{11.7}$$

and

$$\rho_{M-1} = \frac{1}{2} \sum_{m=1}^{M-1} \zeta_m. \tag{11.8}$$

Recursion formulas (11.6) for the direct scattering transform are analogous to the recursion relation (5.6) for the Fourier transform. Like (5.6), execution of (11.6) requires M^2 operations as one iterates over space x and wavenumber κ. Note further that the recursion relations for $[F_m(z), G_m(z)]$ and $[F_m(1/z), G_m(1/z)]$ do not depend on one another. Since we need only matrix elements M_{11} and M_{12} to compute the DST, and since by (11.5), we need only $F_{M-1}(z)$ and $G_{M-1}(z)$, then to calculate the infinite-line DST spectrum it is not necessary to compute the $[F_{M-1}(1/z), G_{M-1}(1/z)]$.

A note of caution is necessary when using (11.6). It is tempting to factor s_m from the matrix of (11.6) and to lump this with the factors $z^{\pm\rho_{M-1}}$ of (11.5). For the discrete spectrum ($\kappa = iK_n$) this procedure can result in ill-conditioning of the numbers and can lead to large roundoff errors and subsequently to numbers outside the range of most computers. Equation (11.6) as written, however, is well-behaved and provides an efficient algorithm for finding the DST spectrum (see II for further details).

12. Behavior of the DST Algorithm in the Small-Amplitude Limit

The purpose of this section is to demonstrate that the direct scattering transform for a discrete wave form as given by the recursion scheme (11.5)–(11.8) reduces to the discrete Fourier transform (6.1) as the wave amplitude becomes small. The results we seek (in the absence of solitions) are given by (4.6) and (4.7) appropriately discretized (rectangular approximation) for the wave pulse (9.1)

$$a(k) \cong 1 + \frac{i\lambda}{k} \sum_{m=0}^{M-1} \eta_m \, \Delta x \tag{12.1}$$

$$b(k) \cong \frac{i\lambda}{k} \Delta x \left[\frac{\sin(k\,\Delta x/2)}{(k\,\Delta x/2)} \right] \sum_{m=0}^{M-1} \eta_m \exp(ikx_m). \tag{12.2}$$

We seek to recover (12.1), (12.2) from (9.7), (9.11), (10.7)–(10.10), and (11.5)–(11.8) to demonstrate that this solution has the appropriate linear Fourier transform limit and to discover under what conditions this limit can occur. The results also provide additional insight into the structure of the DST algorithm.

We first set

$$z_0 = \exp(ik\,\Delta x) = z^k, \qquad z = \exp(i\,\Delta x) \tag{12.3}$$

and then write the coefficients $a(k)$ and $b(k)$ in terms of $F_{M-1}(z)$, $G_{M-1}(z)$ as (use (11.5) in (10.7), (10.10), (9.7), and (9.11)):

$$a(k) = [z_0^{M-1/2} z^{-\rho_{M-1}} F_{M-1}(z)]^{-1} \tag{12.4}$$

$$b(k) = \frac{-z_0^{-M+1/2} G_{M-1}(z)}{F_{M-1}(z)}. \tag{12.5}$$

We now make the following small amplitude expansions:

$$\zeta_m \cong k(1+2\Delta_m)/2; \qquad \Delta_m = \lambda\eta_m/k^2 \tag{12.6}$$

$$s_m \cong 1+\Delta\eta_m; \qquad \Delta\eta_m = \Delta_{m+1}-\Delta_m \tag{12.7}$$

$$d_m \cong -\Delta\eta_m. \tag{12.8}$$

Note that Δ_m of (12.6) is the "spectral Ursell number" (4.9) which intuitively must be small to recover the Fourier limit. Eqs. (12.6)–(12.8) lead to an approximate expression for (11.8),

$$\rho_{M-1} \cong \frac{1}{2}k(M-1)+\frac{\lambda}{k}\sum_{m=1}^{M-1}\eta_m, \tag{12.9}$$

and to first order the recursion relations (11.6) become

$$\begin{pmatrix} F_m(z) \\ G_m(z) \end{pmatrix} \cong \begin{pmatrix} 1+\Delta\eta_m & -\Delta\eta_m z_0 \\ -\Delta\eta_m & (1+\Delta\eta_m)z_0 \end{pmatrix} \begin{pmatrix} F_{m-1}(z) \\ G_{m-1}(z) \end{pmatrix}. \tag{12.10}$$

Upon iterating (12.10) beginning with $F_0 = 1$ and $G_0 = 0$ (retaining only terms at first order in amplitude), we find the following expressions for F_{M-1}, G_{M-1}:

$$F_{M-1} \cong 1+\sum_{m=1}^{M-1}\Delta\eta_m \tag{12.11}$$

$$G_{M-1} \cong -z_0^{M-1}\sum_{m=1}^{M-1}\Delta\eta_m z^{-m}. \tag{12.12}$$

If we take (as mentioned previously in Section 9) $\eta_0 = \eta_1 = \eta_{M-1} = \eta_M = 0$, then after some manipulation,

$$F_{M-1} \cong 1 \tag{12.13}$$

$$G_{M-1} \cong -z_0^{M-1/2}\left[\frac{i\lambda}{k}\frac{\sin(k\,\Delta x/2)}{(k\,\Delta x/2)}\Delta x\right]\sum_{m=0}^{M-1}\eta_m \exp(-ikx_m). \tag{12.14}$$

Finally (12.13), (12.14) are inserted into (12.4), (12.5) and we find the discrete formulas (12.1), (12.2). Thus the recursive algorithm for the direct scattering transform approaches the Fourier transform (12.1), (12.2) for small amplitude waves. We note that the function $G_{M-1}(z)$ reduces to the Fourier transform, while $F_{M-1}(z)$ degenerates to 1 in the small amplitude limit. The approximate recursion formulas (12.10) may be compared to (5.6) for the discrete Fourier transform. Even in the linear Fourier limit the structure of the direct scattering transform is indeed richer that the structure of the Fourier transform.

13. Summary and Conclusions

In order to develop an algorithm for computing the direct scattering transform of a localized initial wave described by the Korteweg–de Vries equation we have used the discretization procedure shown in Fig. 1. A continuous wave amplitude function $\eta(x, 0)$ (Fig. 1a) is discretized into M points separated by equal intervals Δx (as shown in Fig. 1b). The discrete array is then associated with a piecewise constant function (Fig. 1c), where the discrete points are centered inside each interval Δx. Then the Schroedinger eigenvalue problem (3.2) is solved exactly for this piecewise constant function; the solution may be formulated in terms of the *spectral matrix* $\mathbf{M}(\kappa)$ which is found from the product of M "**T** matrices" (computed for each partition Δx) by (9.3)–(9.6). This formulation is unfortunately dependent upon "exploding exponentials" $\exp(Kx)$ which introduce large roundoff errors and make computation of the discrete spectrum difficult. The problem can be alleviated by reformulating the solution in terms of "delta **T** matrices" which depend on Δx rather than x so that only exponentials of the form $\exp(K\,\Delta x)$ appear; the resultant formulation (10.7)–(10.11) is then computationally reliable and accurate. The final step is to express the $\mathbf{M}(\kappa)$ matrix in terms of recursion relations (11.5)–(11.8); these provide an efficient algorithm for computing the DST spectrum. Some justification for our approach is that: (1) it reduces to well-known discrete Fourier methods in the small amplitude limit; (2) it is compatible with the trapezoidal algorithm for the inverse scattering transform [44]; (3) it provides simple ways to estimate spectral errors in the analysis of noisy experimental data (paper II); (4) it may be extended [70] to the class of spectral problems due to Ablowitz, Kaup, Newell, and Segur [1, 5]; and (5) it may be extended to solve periodic problems as well [19, 20, 32, 38, 70, 71].

Acknowledgments

We acknowledge the continuing support of Professors C. Castagnoli and L. Bergamasco.

References

1. M. J. Ablowitz and H. Segur, *Solitons and the Inverse Scattering Transform* (SIAM, Philadelphia, 1981).
2. J. S. Bendat and A. G. Piersol, *Random Data: Analysis and Measurement Procedures* (Wiley-Interscience, New York, 1971).
3. J. W. Cooley, *Math. Comput.* **15**, 363 (1961); J. W. Cooley and J. W. Tukey, *Math. Comput.* **19**, 297 (1965); J. W. Cooley, P. A. W. Lewis, and P. D. Welch, *IEEE Trans. Audio Electroacoust.* **AU-17**, 77 (1969); R. C. Singleton, *IEEE Trans. Audio Electroacoust.* **AU-17**, 93 (1969).
4. C. S. Gardner, J. M. Greene, M. D. Kruskal, and R. M. Miura, *Phys. Rev. Lett.* **19**, 1095 (1967).
5. M. J. Ablowitz, D. J. Kaup, A. C. Newell, and H. Segur, *Stud. Appl. Math.* **53**, 249 (1974).
6. F. Calogero and A. Degasperis, *Nuovo Cimento B* **32**, 201 (1976); **39**, 1 (1977).

7. G. L. LAMB, *Elements of Soliton Theory* (Wiley, New York, 1980).
8. V. E. ZAKHAROV, S. V. MANAKOV, S. P. NOVIKOV, AND M. P. PITAYEVSKY, *Theory of Solitons: The Method of the Inverse Scattering Problem* (Nauka, Moscow, 1980). [Russian]
9. F. CALOGERO AND A. DEGASPERIS, *Spectral Transform and Solitons: Tools to Solve and Investigate Nonlinear Evolution Equations*, Vol. 1. (North-Holland, Amsterdam, 1982).
10. R. K. DODD, J. C. EILBECK, J. D. GIBBON, AND H. C. MORRIS, *Solitons and Nonlinear Wave Equations* (Academic Press, London, 1982).
11. A. C. NEWELL, *Solitons in Mathematics and Physics* (SIAM, Philadelphia, 1985).
12. A. DEGASPERIS, "Nonlinear Wave Equations Solvable by the Spectral Transform," in *Nonlinear Topics in Ocean Physics*, edited by A. R. Osborne (Elsevier, Amsterdam, 1991).
13. H. P. MCKEAN AND E. TRUBOWITZ, *Comm. Pure Appl. Math.* **29**, 143 (1976).
14. B. A. DUBROVIN AND S. P. NOVIKOV, *Sov. Phys. JETP* **40**, 1058 (1975).
15. Y.-C. MA AND M. J. ABLOWITZ, *Stud. Appl. Math.* **65**, 113 (1981).
16. M. G. FOREST AND D. W. MCLAUGHLIN, *J. Math. Phys.* **23**, 1248 (1982).
17. H. FLASCHKA AND D. W. MCLAUGHLIN, *Prog. Theoret. Phys.* **55**, 438 (1976).
18. H. FLASCHKA, *Phys. Rev. B* **9**, 1924 (1974); *Prog. Theoret. Phys.* **51**, 703 (1974).
19. A. R. OSBORNE AND L. BERGAMASCO, *Nuovo Cimento B* **85**, 2293 (1985).
20. A. R. OSBORNE AND L. BERGAMASCO, *Physica D* **18**, 26 (1986).
21. M. J. ABLOWITZ AND J. LADIK, *J. Math. Phys.* **16**, 598 (1975); **17**, 1011 (1976); *Stud. Appl. Math.* **55**, 213 (1976); **57**, 1 (1977).
22. A. R. OSBORNE, A. PROVENZALE, AND L. BERGAMASCO, *Nuovo Cimento C* **5**, 597 (1982).
23. A. R. OSBORNE, A. PROVENZALE, AND L. BERGAMASCO, *Nuovo Cimento C* **5**, 612 (1982).
24. A. R. OSBORNE, A. PROVENZALE, AND L. BERGAMASCO, *Nuovo Cimento C* **5**, 633 (1982).
25. A. R. OSBORNE, A. PROVENZALE, AND L. BERGAMASCO, *Lett. Nuovo Cimento* **36**, 593 (1983).
26. A. R. OSBORNE, "The Spectral Transform: Methods for the Fourier Analysis of Nonlinear Wave Data," in *Statics and Dynamics of Nonlinear Systems*, edited by G. Benedek, H. Bilz, and R. Zeyher (Springer-Verlag, Berlin, 1983).
27. A. R. OSBORNE, "The Generation and Propagation of Internal Solitons in the Andaman Sea," in *Soliton Theory: A Survey of Results*, edited by A. P. Fordy (Manchester Univ. Press, Manchester, UK, 1990).
28. A. R. OSBORNE, M. PETTI, G. LIBERATORE, AND L. CAVALERI, "Nonlinear Fourier Analysis of Laboratory Generated, Broad-banded Surface Waves," in *Computer Modelling in Ocean Engineering*, edited by B. A. Schrefler and O. C. Zienkeiwicz (Balkema, Rotterdam, 1988), p. 99.
29. A. R. OSBORNE, G. BOFFETTA, E. SEGRE, AND L. CAVALERI, submitted for publication.
30. W. E. FERGUSON, JR., H. FLASCHKA, AND D. W. MCLAUGHLIN, *J. Comput. Phys.* **45**, 157 (1982).
31. A. R. BISHOP AND P. S. LOMDAHL, *Physica D* **18**, 54 (1986); A. R. BISHOP, M. G. FOREST, D. W. MCLAUGHLIN, AND E. A. OVERMAN II, *Physica D* **18**, 283 (1986).
32. A. R. OSBORNE AND E. SEGRE, *Physica D* **44**, 575 (1990); E. R. TRACY, J. LARSON, A. R. OSBORNE, AND L. BERGAMASCO, "The Relationship between the Spectral Theories and the Periodic Korteweg–de Vries and Nonlinear Schroedinger Equations," in *Nonlinear Topics in Ocean Physics*, edited by A. R. Osborne (Elsevier, Amsterdam, 1991); *Physica D* **32**, 83 (1988).
33. N. J. ZABUSKY, *J. Comput. Phys.* **43**, 195 (1981).
34. I. KAY AND H. E. MOSES, *Nuovo Cimento* **2**, 917 (1955).
35. P. M. MORSE AND H. FESHBACH, *Methods of Theoretical Physics* (McGraw-Hill, New York, 1953).
36. J. W. MILES, *Ann. Rev. Fluid Mech.* **12**, 11 (1980).
37. H. SEGUR, *J. Fluid Mech.* **59**, 721 (1973).
38. A. R. OSBORNE, "Nonlinear Fourier Analysis," in *Nonlinear Topics in Ocean Physics*, edited by A. R. Osborne (Elsevier, Amsterdam, 1991).
39. A. R. OSBORNE AND G. BOFFETTA, "A Summable Multiscale Expansion for the KdV Equation," in *Nonlinear Evolution Equations: Integrability and Spectral Methods*, edited by A. Degasperis and A. P. Fordy (Manchester Univ. Press, Manchester, UK, 1990).
40. A. PROVENZALE AND A. R. OSBORNE, *J. Comput. Phys.* **94**, 314 (1991).

41. A. R. OSBORNE AND G. BOFFETTA, *Phys. Fluids A* **1**, No. 7, 1200 (1989).
42. G. BOFFETTA AND A. R. OSBORNE, submitted for publication.
43. K.-C. NG, *J. Comput. Phys.* **16**, 396 (1974).
44. O. H. HALD, *Linear Algebra Appl.* **28**, 99 (1979).
45. B. NUMEROV, *Publ. Obs. Cent. Astrophys. Russ.* **2**, 188 (1933).
46. C. FROESE-FISCHER, *The Hartree–Fock Method for Atoms* (Wiley, New York, 1977).
47. J. M. BLATT, *J. Comput. Phys.* **1**, 382 (1967).
48. B. R. JOHNSON, *J. Chem. Phys.* **67**, 4086 (1977).
49. F. Y. HAJJ, *J. Phys. B* **13**, 4521 (1980).
50. D. F. MAYERS, "Computational Methods in the Differential Equations of Atomic Physics," in *New Directions in Atomic Physics*, edited by E. U. Condon and O. Sinanoglu (Yale Univ. Press, New Haven, 1972), Vol. I.
51. E. A. BURKE, *J. Math. Phys.* **21**, 1366 (1980).
52. J. CANOSA AND R. G. DE OLIVEIRA, *J. Comput. Phys.* **5**, 88 (1970).
53. R. G. GORDON, *J. Chem. Phys.* **51**, 14 (1969).
54. M. DUFF, H. RABITZ, A. ASKAR, A. CAKMAK, AND M. ABLOWITZ, *J. Chem. Phys.* **72**, 1543 (1980).
55. M. D. MIKHAILOV AND N. L. VULCHANOV, *J. Comput. Phys.* **50**, 323 (1983).
56. L. COLLATZ, *The Numerical Treatment of Differential Equations* (Springer-Verlag, Berlin, 1966).
57. D. J. LOCKER, *J. Phys. Chem.* **75**, 1756 (1971).
58. B. W. SHORE, *J. Phys. B* **6**, 1923 (1973).
59. J. P. CHESIEK, *J. Chem. Phys.* **49**, 3772 (1968).
60. B. W. SH-NE, *J. Chem. Phys.* **59**, 6450 (1973).
61. D. O. HARRIS, G. ENGERHOLM, AND W. GWINN, *J. Chem. Phys.* **43**, 1515 (1965).
62. A. S. DICKINSON AND R. P. CERTAIN, *J. Chem. Phys.* **49**, 4209 (1968).
63. M. D. FEIT, J. A. FLECK, JR., AND A. STEIGER, *J. Comput. Phys.* **47**, 412 (1982).
64. C. SCHWARTZ, *J. Comput. Phys.* **2**, 90 (1967).
65. J. GARY AND R. HELGASON, *J. Comput. Phys.* **5**, 169 (1970).
66. A. S. DICKINSON, *J. Comput. Phys.* **11**, 458 (1973).
67. R. GUARDIOLA AND J. ROS, *J. Comput. Phys.* **45**, 374, 390 (1982).
68. L. D. LANDAU AND E. M. LIFSHITZ, *Quantum Mechanics* (Pergamon, London, 1958).
69. E. MERZBACHER, *Quantum Mechanics* (Wiley, New York, 1970).
70. G. BOFFETTA AND A. R. OSBORNE, submitted for publication.